

Stress reduction of Cu-doped diamond-like carbon films from ab initio calculations

Xiaowei Li, Peiling Ke, and Aiyi Wang

Citation: *AIP Advances* **5**, 017111 (2015); doi: 10.1063/1.4905788

View online: <http://dx.doi.org/10.1063/1.4905788>

View Table of Contents: <http://scitation.aip.org/content/aip/journal/adva/5/1?ver=pdfcov>

Published by the *AIP Publishing*

Articles you may be interested in

[Protection of Diamondlike Carbon Films from Energetic Atomic Oxygen Degradation Through Sidoping Technology](#)

AIP Conf. Proc. **1087**, 368 (2009); 10.1063/1.3076850

[Thermal conductivity of diamond-like carbon films](#)

Appl. Phys. Lett. **89**, 161921 (2006); 10.1063/1.2362601

[Diamond-like carbon nanocomposite films](#)

Appl. Phys. Lett. **82**, 3526 (2003); 10.1063/1.1576909

[Hydrogen migration in diamond-like carbon films](#)

J. Appl. Phys. **82**, 3791 (1997); 10.1063/1.365741

[Electroluminescence in diamondlike carbon films](#)

Appl. Phys. Lett. **53**, 1880 (1988); 10.1063/1.100381



Goodfellow

metals • ceramics • polymers
composites • compounds • glasses

Save 5% • Buy online
70,000 products • Fast shipping

www.goodfellowusa.com

Stress reduction of Cu-doped diamond-like carbon films from ab initio calculations

Xiaowei Li, Peiling Ke, and Aiyang Wang^a

Key Laboratory of Marine Materials and Related Technologies, Zhejiang Key Laboratory of Marine Materials and Protective Technologies, Ningbo Institute of Materials Technology and Engineering, Chinese Academy of Sciences, Ningbo 315201, P.R. China

(Received 14 December 2014; accepted 29 December 2014; published online 8 January 2015)

Structure and properties of Cu-doped diamond-like carbon films (DLC) were investigated using ab initio calculations. The effect of Cu concentrations (1.56~7.81 at.%) on atomic bond structure was mainly analyzed to clarify the residual stress reduction mechanism. Results showed that with introducing Cu into DLC films, the residual compressive stress decreased firstly and then increased for each case with the obvious deterioration of mechanical properties, which was in agreement with the experimental results. Structural analysis revealed that the weak Cu-C bond and the relaxation of both the distorted bond angles and bond lengths accounted for the significant reduction of residual compressive stress, while at the higher Cu concentration the increase of residual stress attributed to the existence of distorted Cu-C structures and the increased fraction of distorted C-C bond lengths. © 2015 Author(s). All article content, except where otherwise noted, is licensed under a Creative Commons Attribution 3.0 Unported License. [<http://dx.doi.org/10.1063/1.4905788>]

I. INTRODUCTION

Diamond-like carbon (DLC) films are widely investigated due to their unique structures and excellent mechanical, electronic, optical, and magnetic properties,¹ which are not only used as a protective coating in various industrial applications, but also considered in the fields of solar cell, magnetic disk storage devices, medical application and so on.²⁻⁴ However, high level of residual compressive stress limits the films thickness to a few tens of nanometers and is the major drawback to their technological applications. Recently, it has been shown experimentally that an effective way to avoid the high residual stress of DLC films is the introduction of a small amount of Cu during the growth process. For example, Dwivedi *et al.*⁵ reported that Cu containing DLC (Cu-DLC) films prepared by PECVD process exhibited extremely low residual stress (<1 GPa) than pure-DLC films, and they revealed that Cu incorporation enhanced the graphite-like sp^2 bonding, which resulted in the reduction of residual stress. Chen *et al.*⁶ also found that embedding Cu nanoparticles in the DLC matrix reduced the film stress to 0.7 GPa, but they suggested that the weak bonding between Cu and C that allowed sliding at the grain(Cu)-matrix(C) interface may be a possible mechanism of reduced stress. It is well noted that the residual compressive stress is strongly dependent on the distorted atomic bonds in amorphous carbon structure. However, the addition of metal atoms brings the complexity of structure. Especially, due to the limited experimental characterization of the atomic bond structure, the effect of doped metal atoms on the atomic bond structure from the viewpoint of atomic scale is yet to be clarified, leading to the phenomenological explanation and controversy of stress reduction mechanism.

Theoretical simulation technique provides a robust method for in-depth insight of the atomic bond structure, and thus clears the stress reduction mechanism for metal-doped DLC (Me-DLC) films. But most of the previous computational results focused on the mechanism of sp^3 bond formation and the dependence of the atomic bond structure on the kinetic energy of the deposited

^aElectronic mail: aywang@nimte.ac.cn



species in pure carbon or hydrocarbon system.⁷⁻⁹ In contrast, computational study on the metal element addition in DLC films is highly limited, especially for the direct simulation of the Me-DLC film growth by classical molecular dynamics (MD) simulation. Recently, we¹⁰ reported the bond characteristics between all transition metal (TM) atoms and C atom by ab initio calculation using tetrahedral bond model, and revealed that as the 3d electrons of doped TM increased, the bond characteristic between the TM and C atoms changed from bonding (Sc, Ti) to nonbonding (V, Cr, Mn, Fe) and finally to antibonding (Co, Ni, Cu), which accounted for the change of total energy caused by distorting the bond angles. Although the previous work provided an explanation for stress evolution from strain energy arising from the distortion of the atomic bond structure, the structural evolution caused by the doped metal atoms is still required in order to clarify the stress reduction mechanism and the relation between the structure and properties.

In this article, we present an ab initio calculation based on density functional theory (DFT) to investigate the structure and properties of Cu-DLC films with different Cu concentrations. Compared with the classical MD methods which require predetermined empirical potential parameters for specified compositions, the superiority of the parameter-free ab initio simulation method is obvious. The radial distribution function (RDF), properties including the residual compressive stress and bulk modulus, and both the bond angle and bond length distributions were evaluated to reveal the dependence of structural properties on Cu concentration and finally clarify the stress reduction mechanism. Results showed that the atomic bond structure was strongly dominated by the concentrations of the doped Cu atoms, which provided the explanations for the changes in the physicochemical properties of Cu-doped DLC films.

II. COMPUTATIONAL METHODS

All the calculations were carried out using Vienna ab initio simulation package (VASP)^{11,12} with a cutoff energy of 500 eV and a generalized gradient approximation (GGA) with the Perdew-Burke-Ernzerhof parameterization.¹³ The initial configuration contained 64 atoms in a simple cubic supercell with constant volume and under periodic boundary conditions throughout the simulation, which has been proved that such system was suitable and accurate to reveal the characteristics of amorphous carbon systems.¹⁴⁻¹⁶ To obtain Cu-DLC systems, a two-step process composed of melt-quenching by ab initio molecular dynamics (AIMD) simulation and geometric optimization by static calculations was used, which has been demonstrated to provide a good description of DLC materials and to reveal the intrinsic relation between the structure and properties.^{14,17,18} During the AIMD simulation, the system was first equilibrated at 8000K for 1ps to become completely liquid and to eliminate its correlation to the initial configuration using a canonical ensemble with a Nose thermostat for temperature-control and a time step of 1 fs, which was confirmed by calculating RDF of the samples; then, the samples were quenched from 8000 to 1 K at cooling rate of 1.6×10^{16} K/s. For the subsequent geometric optimization of amorphous structure, a full relaxation of the atomic positions based on conjugated gradient method¹⁹ was repeated until the Hellmann-Feynman force on each atom was below 0.01 eV/Å, and the self-consistent loop was created using an energy convergence criterion of 10^{-5} eV. The Γ -only k -point was used to sample the Brillouin zone. To check the k -point convergence on amorphous structure, a fully converged calculation with a grid of $4 \times 4 \times 4$ points (64k points) was performed. When the Γ point only was used, compared to a fully converged calculation with 64k points, the absolute error of average binding energy of per atom was found to be accurate to better than 0.004 eV.

In the amorphous structure, Cu concentrations ranged from 1.56 to 7.81 at.%, which corresponded to 1, 2, 3, 4 and 5 Cu atoms in 64-atom systems, respectively. To provide more representative models of the actual Cu-DLC systems than the direct substitution of carbon by metal atoms in the pre-generated pure-DLC networks, Cu atoms were introduced by substituting carbon atoms in the liquid carbon sample at densities of 2.87 or 2.03 g/cm³.^{14,18} Pure-DLC films were also involved for comparison with Cu-doped ones. Then, the RDF, sp^3 content, residual compressive stress, bulk modulus, and the distributions of both the bond angles and bond lengths in various Cu-DLC films were evaluated.

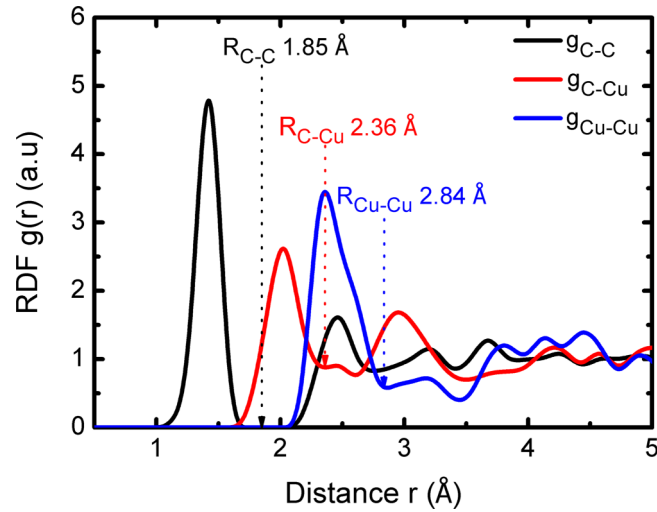


FIG. 1. RDF of Cu-DLC film with high Cu concentration of 39 at.%, in which the inset values are the R_{cut} for C-C, C-Cu, and Cu-Cu bonds.

III. RESULTS AND DISCUSSION

Before characterizing the structure of Cu-DLC films, the RDF, $g(r)$, in the Cu-DLC systems with high Cu concentration (39 at.%) was analyzed first to define whether the Cu atoms were bonded or non-bonded with C atoms, as shown in Fig. 1. The distance to the first minimum in the RDF (inset values of Fig. 1) was set as the cutoff distance, R_{cut} , which was 1.85 Å for C-C, 2.36 Å for C-Cu, or 2.84 Å for Cu-Cu, respectively.²⁰

Figure 2 shows the final morphologies for pure-DLC and Cu-DLC films with the Cu concentrations of 1.56 and 7.81 at.% at 2.87 and 2.03 g/cm³, respectively. Red spheres represent the carbon atoms while yellow spheres are Cu atoms. All the films are amorphous, which will be described later by RDF. For pure-DLC films, it is noted that compared with the pure-DLC film at 2.87 g/cm³,

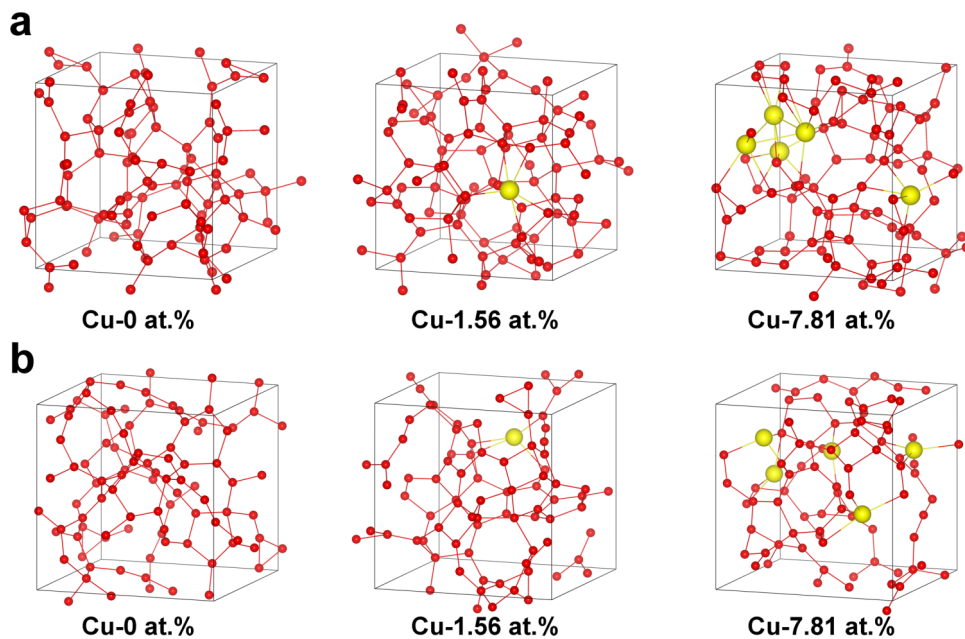


FIG. 2. Atomic structure of Cu-DLC films with Cu concentrations of 0, 1.56, and 7.81 at.% at the densities of (a) 2.87 g/cm³ and (b) 2.03 g/cm³, where red, yellow colors indicate the C and Cu atoms, respectively.

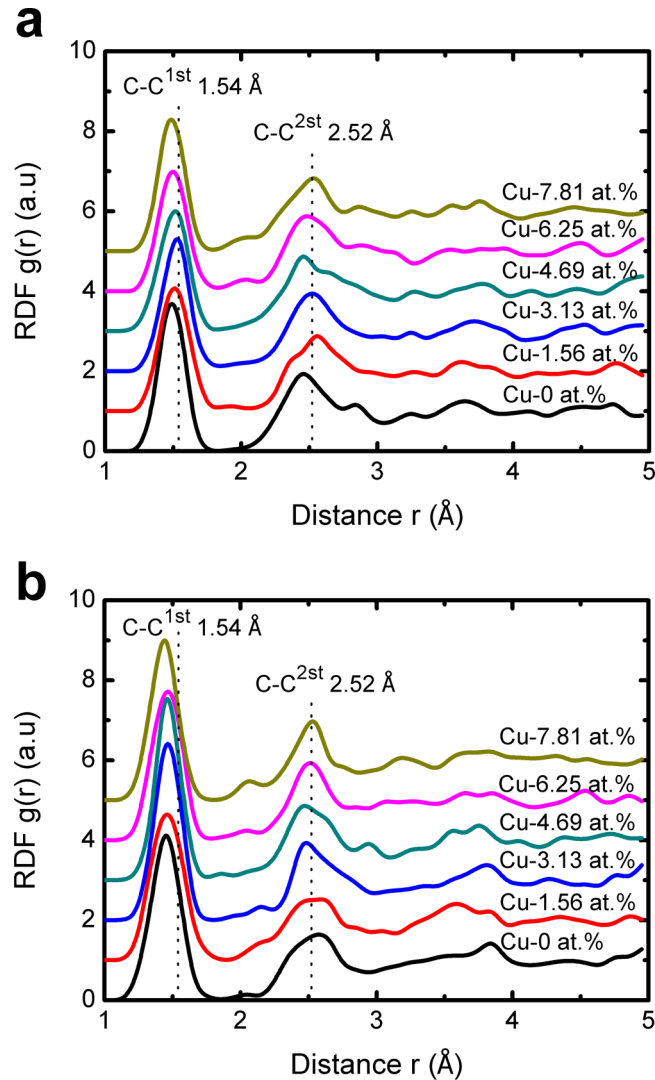


FIG. 3. RDF spectra of Cu-DLC films with different Cu concentrations at (a) 2.87 g/cm³ and (b) 2.03 g/cm³. The vertical dotted lines represent the 1st and 2nd nearest peak positions of crystalline diamond.

the low-density structure of the pure-DLC film (2.03 g/cm³) is looser and contains many planar chains which are weakly cross-linked; as the density changes to 2.87 from 2.03 g/cm³, the sp^3 C content increases to 56.25% from 15.62%. After the addition of Cu, the sp^3 hybridized structure with the Cu content increases gradually for each case because the doped Cu atoms could interact with many C atoms around the doped position; when the Cu concentration in the Cu-DLC film at 2.87 g/cm³ is 7.81 at.% (Fig. 2(a)), the sp^3 C content is 70.31%. Most importantly, it shows that the Cu atoms in the films with high Cu concentration could cluster with each other. Li *et al.*¹⁰ revealed that the bond characteristic between Cu and C atoms was antibonding, which significantly weakened the bond strength and the stability of the system, and Chen *et al.*⁶ also clarified that Cu bonded very weakly with carbon and did not form a carbide phase. Therefore, the Cu metallic clusters can be easily formed in a carbon-based matrix.

Figure 3 shows the RDF spectra of pure-DLC and Cu-DLC films with different Cu concentrations, in which the vertical dotted lines represent the 1st and 2nd nearest peak positions of crystalline diamond. For each case, the film shows the typical amorphous characteristic that is long-range disorder and short-range order. First, for pure-DLC films, the 1st C-C nearest neighbor peak with increasing the density is displaced from 1.46 Å at 2.03 g/cm³ to 1.50 Å at 2.87 g/cm³, which is dependent on the

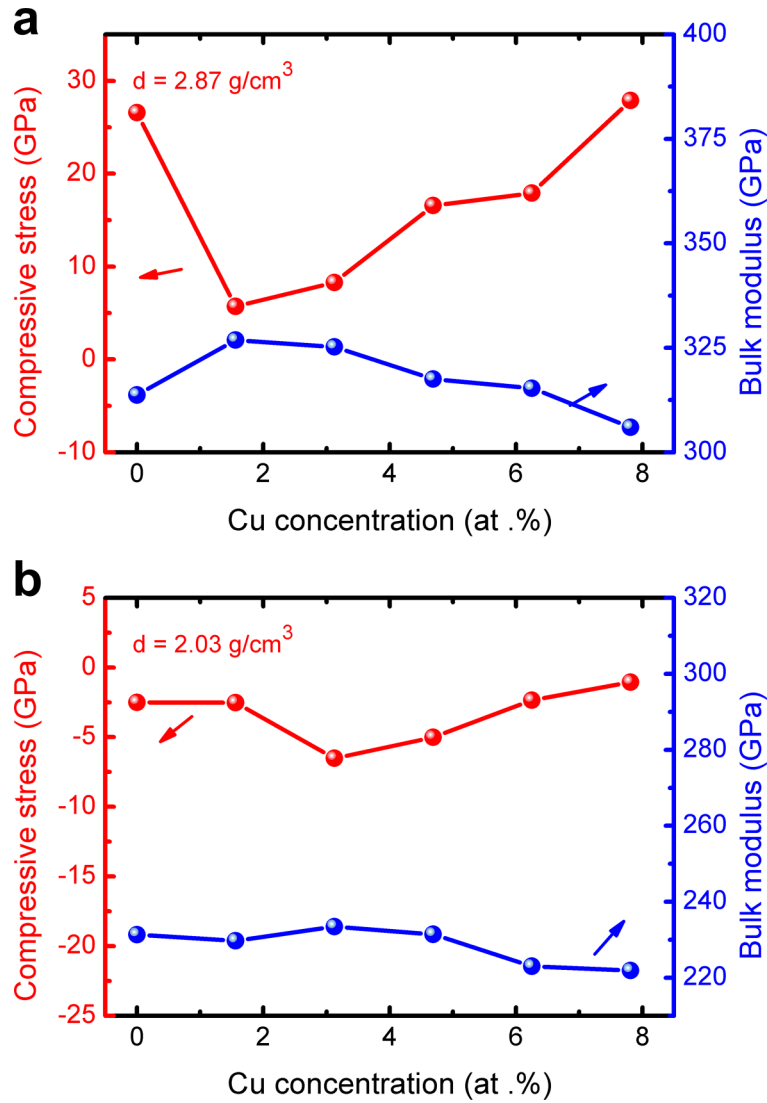


FIG. 4. Compressive stress and bulk modulus of Cu-DLC films as a function of Cu concentrations at densities of (a) 2.87 g/cm³ and (b) 2.03 g/cm³.

hybridization ratio. In addition, the RDF of pure-DLC films from this calculations is in agreement with the previous experimental^{21,22} and theoretical results,^{14,16,23–26} suggesting that the simulated results reflect the nature of real system. The 1st peak is known to be related to the atomic bond lengths, and the 2nd peak has correlation with both the bond angles and bond lengths. However, after doping Cu into DLC films, the positions of the 1st and 2nd nearest neighbor peaks of the Cu-DLC films at 2.87 or 2.03 g/cm³ are deviated from that of pure-DLC films, which demonstrates the evolution of the atomic bond structure including bond angles and bond lengths.

Figure 4 presents the dependence of the calculated residual compressive stress and bulk modulus on the Cu concentrations. The stress, σ , and bulk modulus, B , are computed by the equations

$$P = \frac{P_{xx} + P_{yy} + P_{zz}}{3} \quad (1)$$

$$B = -V \frac{dP}{dV} \quad (2)$$

$$\sigma = \frac{3}{2}P \quad (3)$$

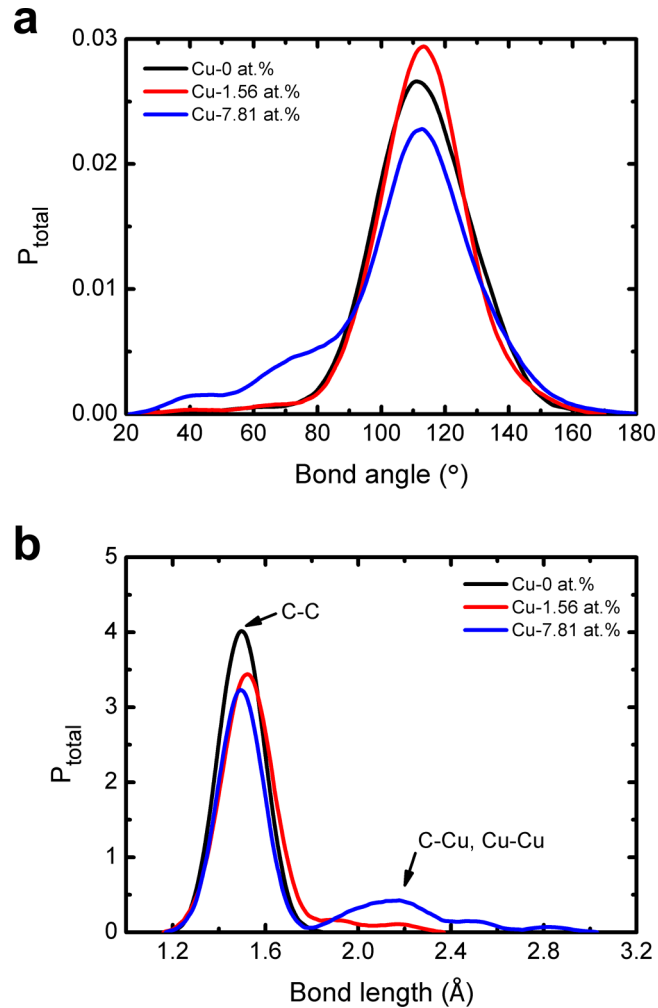


FIG. 5. Total bond angle and length distribution functions of Cu-DLC films at 2.87 g/cm³ (a) total bond angle distribution being composed of the bond angle distributions for all combinations. (b) Total bond length distribution being composed of C-C, C-Cu, and Cu-Cu bond lengths.

where P is the hydrostatic pressure, P_{xx} , P_{yy} and P_{zz} are the diagonal components of the stress tensor, V is the system volume, B is the bulk modulus; the pressure, P , is converted to the biaxial stress, σ , by multiplying the pressure by a factor of 1.5, according to the method of McKenzie (Eqs.(3)).^{27,28} The pure-DLC film at 2.87 g/cm³ shows a high residual compressive stress of about 26.6 GPa, while the tensile stress of about 2.5 GPa is generated in the low-density pure-DLC film (2.03 g/cm³). With introducing Cu atoms into the DLC films at 2.87 g/cm³ as illustrated in Fig. 4(a), the compressive stress with the Cu concentrations decreases drastically and then increases; when the Cu concentration is 1.56 at.%, the minimal residual compressive stress of approximately 5.7 GPa is obtained, which is reduced by 78.5% compared with the pure-DLC film; as the Cu concentration reaches up to 7.81 at.%, the compressive stress increases to 27.9 GPa. Similar behavior for the residual stress with Cu concentrations have also been proved in experiment.⁶ Besides, Fig. 4(a) also reveals that the addition of Cu (1.56~7.81 at.%) causes the bulk modulus decreasing gradually. This attributes to the existence of soft Cu cluster which breaks up the continuity of the hard carbon network. However, in the Cu-DLC films at 2.03 g/cm³ (Fig. 4(b)), the tensile stress is dominate, so the negative value of compressive stress is obtained, which also decreases slightly and then increases; at the Cu concentration of 3.13 at.%, the stress is -6.5 GPa, and the change of bulk modulus is similar to that at 2.87 g/cm³.

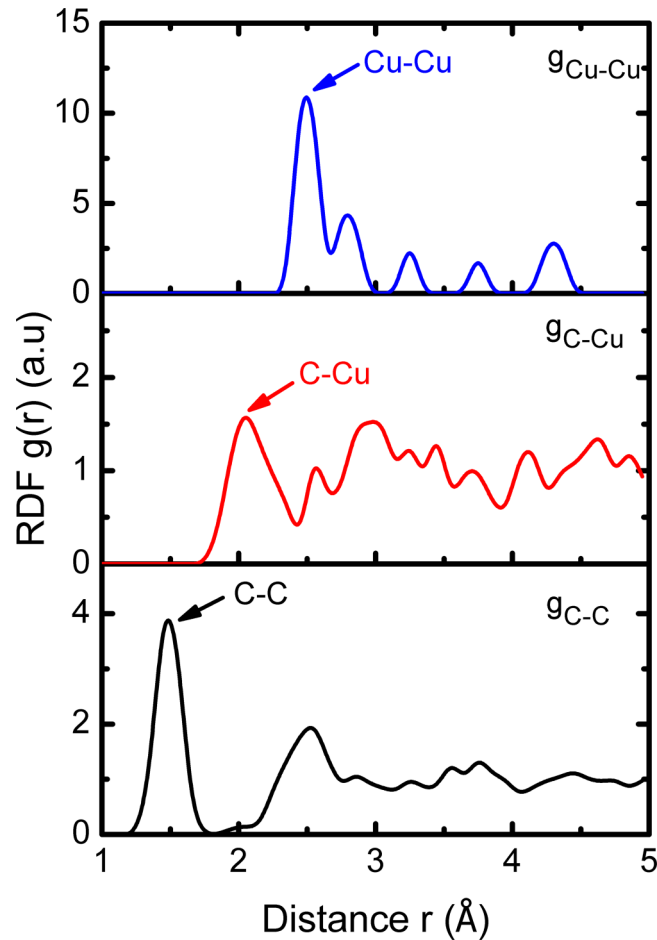


FIG. 6. Decomposed RDF spectra of g_{C-C} , g_{C-Cu} and g_{Cu-Cu} in Cu-DLC film with Cu concentration of 7.81 at.% and density of 2.87 g/cm^3 .

In order to gain insight into the structural evolution and reveal the stress reduction mechanism caused by Cu doping, we investigated the atomic bond structure of Cu-DLC films. Taking the Cu-DLC films with the density of 2.87 g/cm^3 for example to explore the relation between the atomic bond structure and the significant reduction of residual stress (Fig. 4), Figure 5 shows the total bond angle and length distributions for pure-DLC and Cu-DLC films with the Cu content of 1.56 and 7.81 at.%, respectively, in which the total bond angle distribution (Fig. 5(a)) is composed of the bond angle distributions for all combinations and the total bond length distribution (Fig. 5(b)) consists of C-C, C-Cu, and Cu-Cu bond lengths. Fig. 5(a) shows that with the increase of Cu concentration, the peak value of the total bond angle distribution decreases and the peak width shifts toward the small angles obviously, which are induced by the existence of the bond angles containing Cu and C atoms; a small and wide peak located at around 2.17 \AA is generated in the total bond length distribution (Fig. 5(b)). Figure 6 gives the RDF spectra of Cu-DLC film with the Cu content of 7.81 at.%, which is decomposed into partial contributions from the C-C, C-Cu and Cu-C. It obviously proves that the small peak in Fig. 5(b) originates from C-Cu and Cu-Cu bonds because it is longer than C-C bond.

Li *et al.*²⁹ revealed that the distortion of both the bond angles ($<109.5^\circ$) and bond lengths ($<1.42 \text{ \AA}$) of the carbon network resulted in the high level of residual compressive stress. Thus, the C-C-C bond angles and C-C bond lengths in Cu-DLC films were further focused on, respectively, which are illustrated in Fig. 7. The equilibrium bond angle of graphite is 120° and the diamond one is 109.5° (the black dotted lines of Fig. 7(a)); the equilibrium bond length of graphite is 1.42 \AA and the diamond one is 1.54 \AA (the red dotted lines of Fig. 7(b)). It can be found that when the Cu concentration increases from 0 to 1.56 at.%, the populations of both the highly distorted bond

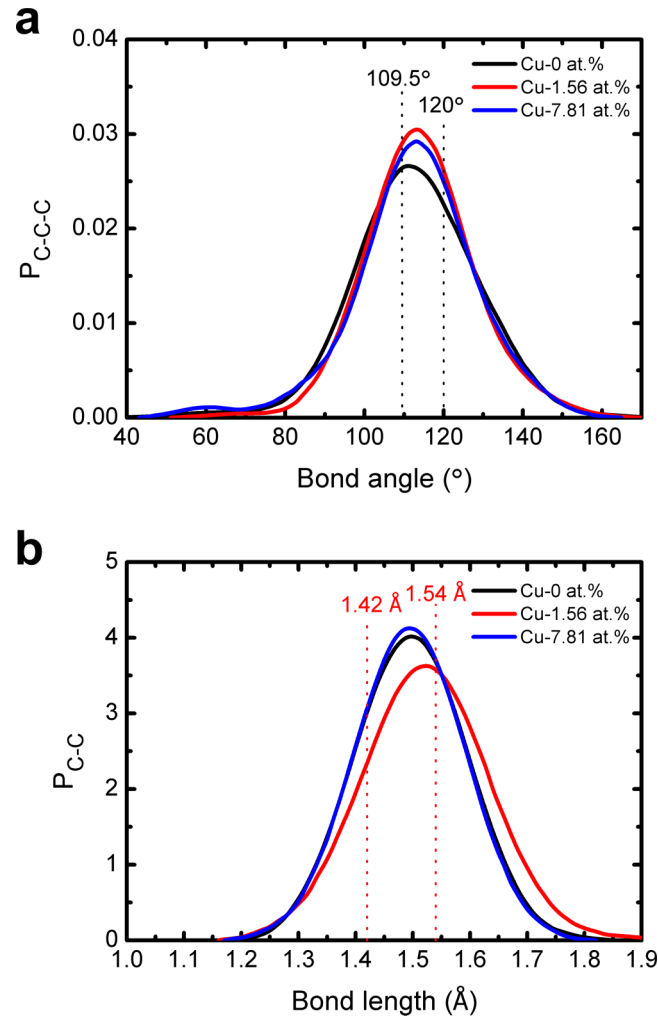


FIG. 7. (a) C-C-C bond angle distribution, P_{C-C-C} , in which black dotted lines represent the stable bond angle of 120° for graphite and the one of 109.5° for diamond. (b) C-C bond length distribution, P_{C-C} , in which red dotted lines represent the stable bond length of 1.42 \AA for graphite and the one of 1.54 \AA for diamond.

lengths smaller than 1.42 \AA and the bond angles smaller than 109.5° decrease simultaneously by comparing with the pure-DLC film, which implies that doping a small amount of Cu into DLC films could effectively relax the distorted bond structure of carbon matrix, leading to the obvious reduction of residual compressive stress. In previous, we have found that the bond characteristics of antibonding between Cu and C atoms was formed, resulting in the reduction of the strength of the system.¹⁰ Therefore, it can be concluded that the fundamental mechanism of residual stress reduction caused by Cu doping mainly attributes to the weak Cu-C bond and the decreased fraction of both distorted bond angles and bond lengths. However, at higher Cu concentration of 7.81 at% the fraction of distorted C-C bond lengths increases remarkably, and many distorted C-Cu and Cu-Cu structures are also formed due to the higher Cu concentration, so these could account for the increase of residual compressive stress (Fig. 4). The same change of atomic bond structure with Cu concentrations is also noted in the Cu-DLC films with the density of 2.03 g/cm^3 .

IV. CONCLUSION

Ab initio calculations based on DFT were employed to study the effects of Cu doping (1.56~7.81 at.% Cu concentrations) on the structure and properties of Cu-DLC films. When the Cu concentration

increased from 0 to 1.56 at.%, the residual compressive stress in Cu-DLC film at 2.87 g/cm³ was reduced from 26.6 to 5.7 GPa; with further increasing Cu concentration to 7.81 at.%, the residual stress increased. At the density of 2.03 g/cm³, the similar behavior of stress with the Cu concentration was also observed. In addition, the bulk modulus was deteriorated for each case due to the existence of soft Cu cluster. By analyzing the atomic bond structure, it revealed that the stress reduction caused by Cu attributed to the weak Cu-C bond characteristic and the relaxation of both the distorted bond angles and bond lengths, while at higher Cu concentration of 7.81 at.% the increase of distorted C-C bond lengths and the existence of distorted C-Cu structures were the key factors to result in the increase of residual stress.

ACKNOWLEDGMENTS

This research was supported by the State Key Project of Fundamental Research of China (2013CB632302), National Natural Science Foundation of China (51402319), China Postdoctoral Science Foundation (2014M551780) and Ningbo Municipal Natural Science Foundation (2014A610001).

- ¹ J. Robertson, *Mater. Sci. Eng.* **37**, 129 (2002).
- ² A. H. Lettington, *Carbon* **36**, 555 (1998).
- ³ J. Brand, R. Gadow, and A. Killinger, *Surf. Coat. Technol.* **180-181**, 213 (2004).
- ⁴ C. Casiraghi, J. Robertson, and A. C. Ferrari, *Mater. Today* **10**, 44 (2007).
- ⁵ N. Dwivedi, S. Kumar, H. K. Malik, C. Sreekumar, S. Dayal, C. M. S. Rauthan, and O. S. Panwar, *J. Phys. Chem. Solids* **73**, 308 (2012).
- ⁶ C. C. Chen and F. C. N. Hong, *Appl. Surf. Sci.* **242**, 261 (2005).
- ⁷ B. Zheng, W. T. Zheng, S. S. Yu, H. W. Tian, F. L. Meng, Y. M. Wang, J. Q. Zhu, S. H. Meng, X. D. He, and J. C. Han, *Carbon* **43**, 1976 (2005).
- ⁸ E. Neyts, A. Bogaerts, R. Gijbels, J. Benedikt, and M. C. M. van de Sanden, *Diamond Relat. Mater.* **13**, 1873 (2004).
- ⁹ B. A. Pailthorpe, *J. Appl. Phys.* **70**, 543 (1991).
- ¹⁰ X. Li, K. R. Lee, and A. Wang, *J. Comput. Theor. Nanos.* **10**, 1688 (2013).
- ¹¹ G. Kresse and J. Furthmüller, *Comp. Mater. Sci.* **6**, 15 (1996).
- ¹² G. Kresse and J. Furthmüller, *Phys. Rev. B* **54**, 11169 (1996).
- ¹³ J. P. Perdew, K. Burke, and M. Ernzerhof, *Phys. Rev. Lett.* **77**, 3865 (1996).
- ¹⁴ B. Zheng, W. T. Zheng, K. Zhang, Q. B. Wen, J. Q. Zhu, S. H. Meng, X. D. He, and J. C. Han, *Carbon* **44**, 962 (2006).
- ¹⁵ F. Alvarez, C. C. Díaz, R. M. Valladares, and A. A. Valladares, *Diamond Relat. Mater.* **11**, 1015 (2002).
- ¹⁶ N. A. Marks, D. R. McKenzie, B. A. Pailthorpe, M. Bernasconi, and M. Parrinello, *Phys. Rev. B* **54**, 9703 (1996).
- ¹⁷ M. M. M. Bilek, D. R. McKenzie, D. G. McCulloch, and C. M. Goringe, *Phys. Rev. B* **62**, 3071 (2000).
- ¹⁸ A. Gambirasio and M. Bernasconi, *Phys. Rev. B* **60**, 12007 (1999).
- ¹⁹ M. J. Gillan, *J. Phys.: Condens. Matter.* **1**, 689 (1989).
- ²⁰ R. Haerle, G. Galli, and A. Baldereschi, *Appl. Phys. Lett.* **75**, 1718 (1999).
- ²¹ F. Li and J. S. Lannin, *Phys. Rev. Lett.* **65**, 1905 (1990).
- ²² K. W. R. Gilkes, P. H. Gaskell, and J. Robertson, *Phys. Rev. B* **51**, 12303 (1995).
- ²³ D. G. McCulloch, D. R. McKenzie, and C. M. Goringe, *Phys. Rev. B* **61**, 2349 (2000).
- ²⁴ N. A. Marks, D. R. McKenzie, B. A. Pailthorpe, M. Bernasconi, and M. Parrinello, *Phys. Rev. Lett.* **76**, 768 (1996).
- ²⁵ G. Galli, R. M. Martin, R. Car, and M. Parrinello, *Phys. Rev. Lett.* **62**, 555 (1989).
- ²⁶ G. Galli, M. M. Richard, C. Roberto, and P. Michele, *Phys. Rev. B* **42**, 7470 (1990).
- ²⁷ D. R. McKenzie, D. Muller, and B. A. Pailthorpe, *Phys. Rev. Lett.* **67**, 773 (1991).
- ²⁸ N. A. Marks, *Phys. Rev. B* **56**, 2441 (1997).
- ²⁹ X. Li, P. Ke, H. Zheng, and A. Wang, *Appl. Surf. Sci.* **273**, 670 (2013).